Influence of Particle-Size Distribution on Entrainment Solid Rate in Fluidized Bed

A. M'chirgui, L. Tadrist, and J. Pantaloni
Institut Universitaire des systèmes Thermiques Industriels (IUSTI),
CNRS-UMR 139 Faculté des Sciences de St-Jérôme, 13397 Marseille Cedex 20 France

Numerous studies undertaken recently to gain increased insight into the dynamics of granular systems emphasize that in vibrating beds, particle collisions produce convection and turbulence. However, a bed composed of particles (such as sand) and fluidized by an upward fluid flow (such as air) presents more complex phenomena, given the existence of hydrodynamic interactions (Davidson et al., 1985).

The upward flow of air through the bed of particles produces a fixed bed at low flow rates, but at higher rates, the solids are lifted and moved in a complex and turbulent pattern, giving rise to a fluidized bed (Kunii and Levenspiel, 1991). At higher velocities, the solids are transported from the riser into the fluid stream. In this case, the flow is diverted into a cyclone where the solids are separated from the air. Then, the particles are recycled via a return loop and then reintroduced into the vessel. In most fluidization applications, the carryover of fine particles in the exit gases is regarded as an inconvenience to be tolerated in exchange for the advantages offered by this technique. In fluidized beds, carryover and reinjection of all bed material is essential.

Fluidized-bed technology has progressed rapidly in combustion applications. The driving motivation behind this development is its excellent stability and temperature control, even with low grade fuels. This technology offers nearly optimal conditions for effective sulfur capture thanks to precise temperature control and intense mass/energy transfer between particles and gas. Unfortunately, these possibilities have not been fully developed. The solid volume fraction distribution and the solid flux inside the reactor must therefore be recovered if the reaction rates, fluidization quality, and energy transfer are to be controlled. Moreover, the design of solid recovery equipment (such as cyclone trains) requires accurate prediction of the solid circulating rate and the size distribution of entrained solids.

Numerous authors have investigated the influence of the solid characteristics on flow hydrodynamics. Lewis (1962) measured the entrainment rate of solids which are composed of uniform particles. He reported that the entrainment does not become significant until the superficial gas velocity reaches a value considerably greater than the free falling velocity of the particles. This author also investigated the effects of column diameter, particle density, freeboard, and dense bed depth on the circulating solid rate. Entrainment rates were found to depend on a large number of variables. The difference between the magnitude of the superficial gas velocity and the particle terminal velocity is considered to be the major factor influencing the rate of solid entrainment (Wen and Hashinger, 1960). Numerous correlations, based on an elutriation constant, have been proposed for the prediction of the circulating solid rate. These correlations have been derived either for similar sized particles or for very wide particle-size distributions (PSDs). These correlations may, however, prove inaccurate when used outside the experimental conditions for which they were developed. There is virtually no information describing the effect of PSD on the fluid dynamics of circulating fluidized beds. Sun and Grace (1992) have recently conducted a number of experiments on transitions between different fluidization regimes. They used distributions that presented roughly the same Sauter diameters with different widths. The results indicated that the amplitude and the frequency of pressure fluctuations are both influenced by particle-size distribution, as is the transition between fluidization regimes.

The present study was undertaken to gain increased insight into the effect of PSD on the entrainment in circulating fluidized beds. In this article, the experimental results show the influence of the PSD on the circulating solid rate.

Our experimental apparatus is shown in Figure 1. The main system consists of: (a) a riser column (1) with a 100 mm $\times$ 100 mm square cross section, and a height of 1,200 mm; (b) a cyclone separator (2) placed at the outlet of the column; (c) a solid storage hopper; (d) an Archimedes screw driven by an electric motor (3). The scale of the riser was chosen in respect of the dimensionless hydrodynamic parameters proposed by Glicksman (1994).

The air is sucked through a perforated plate (30% of free area) which serves as a fast air distributor to the bed. Beneath this plate, there is a homogenization system composed of cylindrical tubes which maintain the gas flow inside the riser symmetrical. The carrying gas rate is measured by a gas flow counter located between the pump and the cyclone inlet. The riser, the cyclone, and the buffer riser are made of Pyrex to allow visual observation.

The circulating solid rate through the riser (and hence the

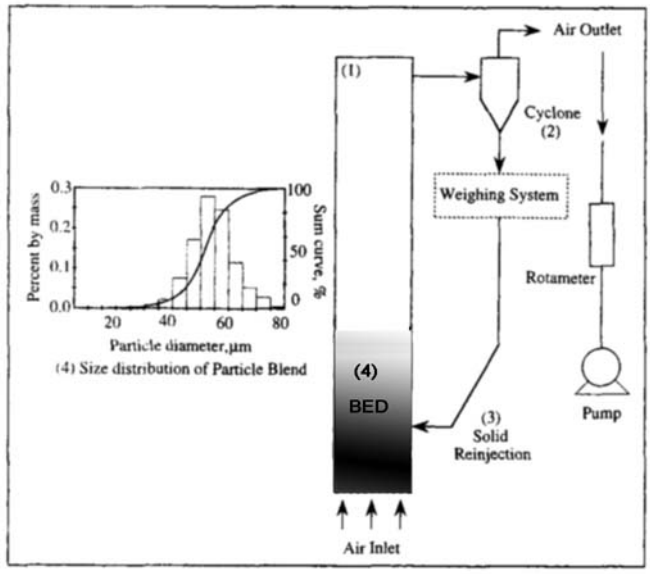

Figure 1. Experimental setup and a sample of the size distribution spectrum of the powder blends.

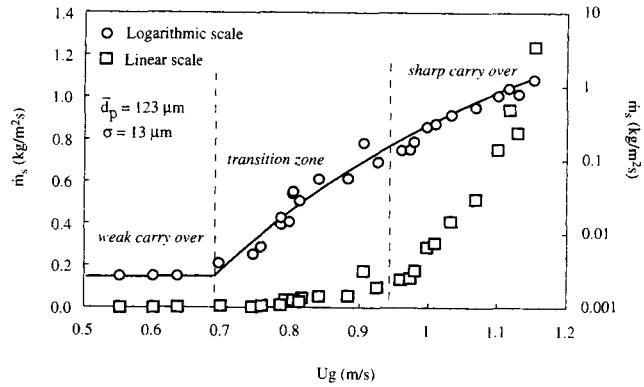

Figure 2. Solid entrainment rate vs. superficial gas velocity.

Distinct carryover states are indicated.

mass-flow rate of solids) is measured by diverting the flow from the cyclone outlet into a weighing container placed on two force transducers. The flow is then sent into the buffer hopper through a pneumatically-controlled valve. The solid rate is determined by closing the hopper's pneumatic outlet valve and monitoring the weight increase (force transducers) at suitable intervals, thus maintaining a steady state in the riser. Operating conditions are recorded, and a steady state was assumed to have been reached when the time-averaged pressure signal and injected air rate have fairly stable values.

The solids used are spherical glass particles with a material density of 2,400 kg/m^3. The PSDs are chosen according to the classification presented by Geldart (1979). Figure 1 shows a sample of the PSD function for the powder blends used in this study. Each PSD is characterized by a volume-surface mean diameter (Sauter diameter) and a standard deviation (distribution breadth). Various PSD are used under experimental conditions with different Sauter diameters and standard deviations.

The fluidization of solid distributions progresses through macroscopically distinct regimes of solid carryover as the gas flow increases. These transitions in Figure 2 show the general increase in the net solid entrainment flux from the riser as the gas flow increases. A number of published correlations describe this evolution using exponential functions of the superficial gas velocity (Kunii and Levenspiel, 1991). The detailed analysis of these profiles led us to present this variation on a semilogarithmic scale (Figure 2). In this representation, the variation of the circulating solid rate is not linear over the entire scale of the superficial gas velocity studied. The behavior of this flow parameter is apparently more complex. Three ranges presenting different carryover behavior can, however, be distinguished.

The first range is characterized by a low particle carryover rate. The mean upward gas velocity is less than the terminal velocity of most particles in the bed. At the outlet of the riser, we observe a small quantity of solids presenting very weak concentrations. The visualized flow pattern indicates that the flow in this first range is governed by the bubbling phenomenon. In this case, we observe the formation of bubbles (or pockets of air) which rise through the dense bed, bursting through its surface, and projecting agglomerates of particles into the space above. This first range ends at a superficial gas velocity U_{g1} (m/s).

The third range is observed for relatively high superficial gas velocities (that is, greater than most terminal velocities of the particles in the bed). The carryover law in this range can be approximated by a strongly sloping linear function, which indicates a significant increase in the net particle flux with additional increase in gas velocity. This range corresponds to the formation of the fast fluidization regime characterized by higher solid concentrations along the riser. The superficial gas velocity U_{g2} (m/s) corresponds roughly to the beginning of this third carryover range.

Between the ranges of weak and strong solid carryover, we observe a third range called the transition range. The solid carryover law can be approximated by a linear curve as a function of the superficial gas velocity in this range. The slope of this curve is greater than in the other two ranges. In the first and third ranges, the breadth of the particle-size distribution does not play a major role in the mechanisms that govern the carryover of solids out of the riser. In the first state, hardly any particle classes are carried out of the column, whereas in the third state all classes are carried out. The breadth of the distribution probably has little influence on the hydrodynamics governing the flow in these two ranges. In the transition range, however, further increase in the superficial gas velocity causes more and more particle classes to be carried over into the freeboard above the bed. The mechanisms governing the entrainment of solids through the riser are thus strongly dependent on both the breadth of the distribution and on the superficial gas velocity. The combination of these two effects may explain the more pronounced and specific increase in the net solid flux in this range.

Measurements of the solid entrainment rate were carried out for two powder blends presenting nearly identical distribution breadths (8 and 11 μm) and different Sauter diameters (53 and 110 μm). Similar variation laws with the superficial gas velocity were obtained for the two powder blends. In earlier studies, the solid entrainment rate has been plotted using different methods to determine the effects of specific

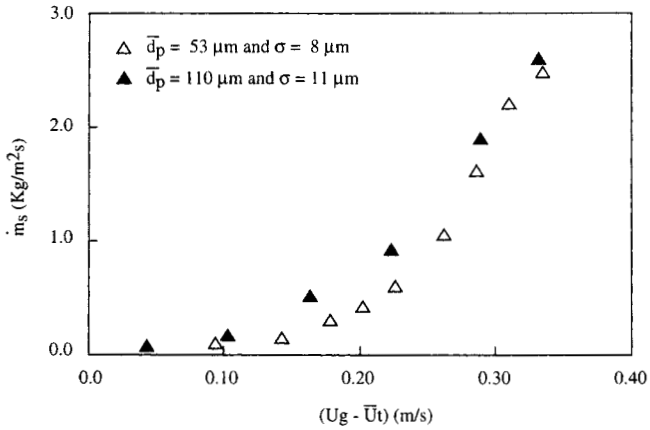

Figure 3. Solid entrainment rate vs. U_g-$\bar{U}_t$ for two PSDs having nearly the same breadth and with different Sauter diameters.

variables. In the present work, we choose to represent the solid entrainment rate as a function of the difference between the superficial gas velocity (m/s) and the free falling velocity of the particle with the Sauter diameter for the given distribution ($U_g - \bar{U}_t$). [$\bar{U}_t$ is the free falling terminal velocity of the median particle ($\bar{d}_p$), m/s calculated using the Schiller and Nauman (1935) drag coefficient. $\bar{d}_p$ is the mean Sauter diameter (volume-surface mean diameter), m.] This velocity difference is called "slip velocity." Figure 3 shows the solid entrainment rate measurements as a function of the slip velocity. In this representation, it is clear that the two profiles merge and present fairly similar variation laws. In this case, the Sauter diameter is not seen to have any influence. This graphical representation effectively shows the influence of the breadth of the solid size distribution.

Figure 4 shows the solid entrainment rate as a function of the slip velocity for three different powder blends (presenting Sauter diameters of 58, 123, and 181 μm, and standard deviations of 6, 13, and 21 μm, respectively). These three solid size distributions have nearly the same relative speed (ratio of the breadth of the distribution to the Sauter diameter). This ratio is equal to 11% ± 1%. The diagram ($\dot{m}_s$ vs. $U_g - \bar{U}_t$) is found to group the three entrainment rate profiles in a common slip velocity range. [$\dot{m}_s$ is the external solid circulating rate or solid entrainment rate (kg/m²s).] It should, however, be noted that these profiles present some gaps; in this representation the order of the curves is reversed. It can be seen that the gap between the profiles increases with the width of the distribution. The solid entrainment rate corresponding to the first powder blend (breadth 6 μm) presents an abrupt variation. The transition range is weakly marked. On the other hand, the profile corresponding to the third powder blend (breadth 21 μm) presents a somewhat more progressive variation. In this case, the transition range is considerably more pronounced. The transition range (and the shape of the solid entrainment rate profile) is strongly dependent on the breadth of the PSD. As the standard deviation of the PSD increases, the transition is more progressive from regimes with weak solid carryover to regimes with considerable solid entrainment.

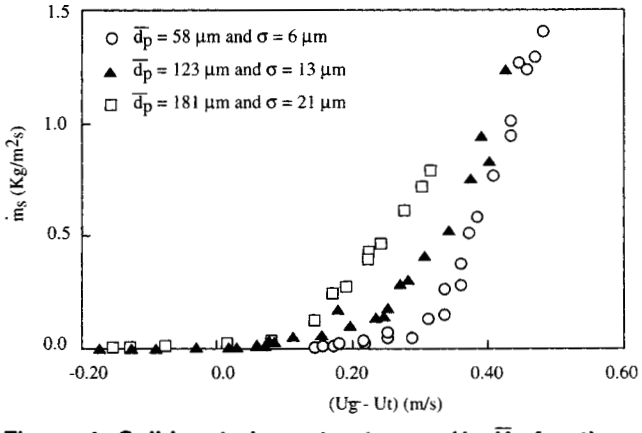

Figure 4. Solid entrainment rate vs. U_g-$\bar{U}_t$ for three PSDs having nearly the same relative spread $\sigma/\bar{d}_p$ (about 11%).

As can be seen in Figure 4, the relative spread ($\sigma/\bar{d}_p$) (maintained at a constant value for the three PSDs tested) does not produce similar laws of solid entrainment. [σ is defined as the breadth of the PSD (standard deviation), m.] Using powder blends with the same breadth and different Sauter diameters, we should obtain the same solid entrainment laws (that is, in the diagram represented by $\dot{m}_s$ vs. $(U_g - \bar{U}_t)$. The breadth of the PSD seems to be a specific parameter of the gas-particle flow.

In conclusion, the analysis of the solid entrainment rate profiles has revealed the existence of a transition flow range between a range characterized by a weak solid carryover and a second range characterized by a considerable solid carryover. The broader the PSD of the solid phase, the more progressive the transition. The physical mechanisms governing the flow in this range are greatly dependent on the PSD and on the superficial gas velocity. The range of superficial gas velocity (where the solid entrainment rate profile is located) depends on the Sauter diameter of the PSD, whereas the shape (and thus the law of variation of the solid carryover) depends only on the width of the PSD. When analyzing the particle-gas flow in a circulating fluidized bed, the granulometric characteristics of the solid phase must be taken into account. The standard deviation of the PSD and the Sauter diameter are most probably independent parameters of the two-phase flow.

Literature Cited

Davidson, J. F., R. Clift, and D. Harrisson, *Fluidization*, Academic Press, London (1985).

Geldart, D., *Gas Fluidisation Technology*, Wiley-Interscience, England (1986).

Glicksman, L. R., M. R. Hyre, and P. A. Farrell, "Dynamic Similarity in Fluidization," *Int. J. Multiphase Flow*, **20**, 331 (1994).

Kunii, D., and O. Levenspiel, *Fluidization Engineering*, 2nd ed., Butterworths, London (1991).

Lewis, W. K., E. R. Gilliland, and P. M. Lang, "Entrainment from Fluidized Beds," *Chem. Eng. Prog. Symp. Ser.*, **58**(38), 65 (1962).

Schiller, L., and A. Z. Nauman, "Über die Grundlegenden Berechnungen bei der Schwerkraftanfbereitung," *Z. Ver. Deut. Ing.*, **77**, 318 (1935).

Sun, G., and J. R. Grace, "Effect of Particle Size Distribution in Different Fluidization Regimes," *AIChE J.*, **38**(5), 716 (1992).

Wen, C. Y., and R. F. Hashinger, "Elutriation of Solid Particles from a Dense-Phase Fluidized Bed," *AIChE J.*, **6**, 220 (1960).

Manuscript received Nov. 13, 1995, and revision received Aug. 12, 1996.